# Electron Transfer of *Shewanella Oneidensis* MR-1 at Clay-Modified ITO Electrode

**Reem Alshehri[1,2*] and Alanah Fitch[1]**

[1]Department of Chemistry and Biochemistry, Loyola University Chicago, Chicago, USA
[2]Department of Chemistry, Taibah University, Al-Ula, KSA
Email: ralshehri1@luc.edu

***Abstract***

The role of structural iron in clays to enhance the electron transfer of *Shewanella Oneidensis* MR-1 was investigated. Three types of clays containing different amounts of iron situated in the octahedral sites have been used to modify the ITO electrodes: nontronite NAu-1, montmorillonite (Wyoming) SWy-1, and synthetic montmorillonite SYn-1. The interaction between bacterial cells and the clay, which modified the ITO electrodes were studied by potential step, cyclic voltammetry, confocal microscope, and scanning electron microscope SEM. Experimental results showed that the current density generated using iron content clays NAu-1 and SWy-1 to modify the ITO electrode was 19 and 3 times higher than that produced using the bare ITO electrode. Also, SEM and confocal microscope proved the increased coverage percentage of the bacterial cells attached to the CME compared to the bare ITO.

***Keywords***

*Shewanella Oneidensis* MR-1, Clay, Modified ITO electrode, MFC

## *1. Introduction*

Electron transfer from organic matter such as glucose or lactate is an important process in the microbial fuel cell. Bacteria work as a catalyst in this process. Microbial fuel cells (MFCs) are a form of a bioreactor, which generates electricity from chemical energy using electrodes. Wastewater treatment, power generation, and biosensors are the most widely used applications for MFCs.[1-4] *Shewanella Oneidensis* MR-1 is a commonly used bacteria in the MFC, which contains cytochromes in its outermost protective membrane, and these cytochromes transport electrons to the nearby electron acceptor. During anaerobic conditions, *S. oneidensis* bacterium reduces the terminal electron acceptors such as Mn (III), Fe (III), nitrate, fumarate, thiosulfate, trimethylamine N-oxide, dimethyl sulfoxide, sulfite, and elemental sulfur.[5]

Various strategies have been established to enhance extracellular electron transfer and energy output capability of MFCs. Most of these attempts are mainly targeted on anode modification[6], substrate sources[7], redox mediators[8], and bioreactor configuration[9]. The anode has a significant impact on the electricity generation performance of MFCs because it is directly contacted with the microorganisms. Lately, the applications of different modified electrodes have been studied such as (CNTs/PAH) ITO electrode[10], $(Fe_2O_3/CS)_4$ ITO electrode[11], and $(PAH/GE)_2$ ITO electrode [12].

Clay minerals are abundantly found in soils, rocks, and sediments, and find application in various fields like pharmaceuticals, pottery, animal feed, wastewater treatment, oil adsorbents, and antibacterial agents.[13-14] Clays are layered materials and consist of tetrahedral silicates (Si-O) and/or octahedral aluminates (Al-O, Al-OH). Clays may consist of one silicate and one aluminate sheet known as a 1:1 layer of clay such as kaolinite. In addition, clays could contain one octahedral sheet sandwiched between two tetrahedral sheets, termed 2:1 layer of clay such as montmorillonite and nontronite .[15] Clay layers contain $Al^{3+}$, $Si^{4+}$, $Mg^{2+}$, and $Fe^{3+}$

in the octahedral and tetrahedral sheets. There are many exchangeable cations between the clay layer such as $Na^+$, $Ca^{2+}$, and $K^+$ which balance the negative charge of clay layers.

Clay-modified electrodes (CME) have attracted the attention of electrochemists worldwide. CMEs are found in a variety of applications, one of which is for sensors.[16-18] The combination of electrodes with clays provide the desired sensitivity, durability, selectivity, and speed of sensors. Moreover, the cost of preparing clay-modified sensors is much less compared to other modified sensors.[19] In the CMEs, electrons transfers occur through the channels by physical diffusion within the clay film.[20-21] Furthermore, electrons hopping through redox-active cation within the clay crystal such as iron is another mechanism of charge transfer in the CME.[22-23] Using clay is also a green initiative, which is the reason some researchers prefer to use it instead of other chemicals, which are toxic. Apart from these benefits, the waste produced by modifying electrodes using clay is negligible; it, therefore, requires the least protocols and permissions.

It has been proven that the existence of iron in the crystal structure of smectite clays, highly impact their physical and chemical properties. These iron atoms are proposed to be involved in the electron transfer process in clay and as a result, influence the response of clay-modified electrodes. For instance, electron transfer of cytochrome c (Cyt-c) at montmorillonite CME was reported by Scheller's research group.[24] Charade and coworkers found that structural iron in clays promoted the direct electron transfer of hemoglobin. Different types of clays were used: nontronite, synthetic montmorillonite, saponite and synthetic montmorillonite containing non-iron impurities. Their findings showed that nontronite, which contains the highest amount of structural iron, significantly enhanced the direct electron transfer of hemoglobin.[25] Oyama and Anson concluded that structural iron in montmorillonite clay mediates the reduction of hydrogen peroxide.[26] Koffi's group was the first one to report the fact that utilizing clay-modified carbon paste electrode to determine for the bacteria in water or blood samples.[27]

However, there is no literature that reports on the possible role of structural iron in the electron transfer of metal-reducing bacteria such as *Shewanella* MR-1 using clay-modified electrode.

In this study, we report the use of structural iron in clay to enhance the direct electron transfer of *Shewanella* MR-1. Clay works as an alternative surface that attracts bacteria and facilitates electron transfer through the iron in the octahedral sheet. For this goal, we have used two ferruginous clays containing different amounts of iron situated in the octahedral sheet and one synthetic montmorillonite containing non-iron. Coverage and porosity of each clay modified ITO electrodes using the anionic electroactive species $[Fe(CN)_6]^{3-}$ were examined. Laser diffraction spectroscopy and light obscuration were used to determine the different particle sizes for the used clays. The clay film thicknesses were measured using the scanning electron microscope. The electrochemical behavior of the clay-modified ITO electrodes was characterized by potential step and cyclic voltammetry in the presence of *Shewanella* MR-1. The changes in bacterial cells attached to the modified electrodes were observed using a confocal microscope and SEM.

## 2. *Materials and Methods*

### *2.1 Materials*

*Shewanella oneidensis* MR-1 microbe were purchased from The Global Bioresource Center (ATCC). Wyoming montmorillonite (SWy-1), nontronite (NAu-1), Synthetic montmorillonite (SYn-1) clays were obtained from the Source Clay Minerals Repository (Purdue University, East Lafayette, Ind., Department of Agronomy). Tryptic Soy Broth, NaCl, KCl, $K_3 Fe(CN)_6$ were purchased from Sigma Aldrich.

### *2.2 Clay-Modified ITO Electrodes*

Each clay suspension was prepared by stirring it into 500 mL deionized water. The total clay concentration in suspension solutions was 5 g/L for each clay. (ITO) Indium tin oxide glass slides (Thin Film Devices, Inc.) were washed, rinsed, dried, and wiped with 70%

isopropyl alcohol, re-dried, and allowed to equilibrate with air. 100, 300, 500 and 800 µL of clay gel were smeared uniformly on ITO with a micropipette and left overnight to air-dry. The film thickness of each film was measured by SEM. Water contact angles were characterized using a Veho discovery camera, and MicroCapture software. Two different samples were measured for each sample and the data were averaged.

### *2.3 Potassium ferricyanide experiment*

NaCl and KCl were prepared in distilled water at different concentrations of 0.05, 0.1, 0.3, 0.5, 0.7, 0.9, and 1.2 M. 3 mM of $[Fe(CN)_6]^{3-}$ solutions were prepared in different concentrations of the NaCl and KCl salts. All solutions were subjected to a $N_2$ purge for 10 minutes before running in the electrochemical cell. The clay film was soaked for 10 minutes by the salt electrolytes solution and then exposed to $[Fe(CN)_6]^{3-}$ solution. The response of CMEs in the presence of different cation electrolytes and $[Fe(CN)_6]^{3-}$ was monitored by cyclic voltammetry. The potential was scanned between 0.8 and - 0.4 V vs. Ag/AgCl at a scan rate of 10 mV/s

### *2.4 Microbial Culture*

S. oneidensis MR-1 from −80 °C freezer stock was inoculated into 100 mL of TSB medium at 30 °C for 12 hours anaerobically. After twelve hours of incubation, the optical density was measured at 650 nm by (VWR UV6300PC double-beam spectrophotometer). The optical density of the culture solution before harvest in the electrochemical cell was 0.3 for all the experiments' conditions. $OD_{650}$ of original culture solution and the culture solution recovered from the electrochemical cell were also measured post-experiment. The resulting cell suspension was centrifuged at 5000 rpm for 10 minutes to pellet cells, and the TSB medium was then replaced with 100 mL of fresh and $N_2$ purged TSB. Three triplicate samples were run on the electrochemical cell on the same day.

### *2.5 Electrochemical Cell*

The electrochemical cell utilized in our laboratory is a single-chamber; it has three-electrodes, which were employed for the electrochemical study. A tin-doped $In_2O_3$ (ITO) substrate on glass slides (surface area of 18 $cm^2$) which had been modified by the clay film was used as the working electrode (WE). Ag/AgCl (NaCl saturated) and a platinum wire were used as reference and counter electrodes, respectively. The cell was positioned such that the ITO (WE) was vertical with the solution pumped from the side and exiting to the top. The positioning was chosen to minimize gravitational deposition of bacteria to the slide. The clay film on the electrode was soaked for 10 min by $N_2$ purged TSB before running in the electrochemical experiment. Immediately after that, a volume of 11 mL of the bacteria culture solution was pumped to the electrochemical cell. For each condition, the current was measured for two hours at the potential of +0.2 V. Then, cyclic voltammetry obtained at +0.2 V initial and final potential while the switching potential was at -0.5 V at a 5 mV/s scan rate. Epsilon EC was used for the electrochemical experiments.

### *2.6 Confocal Microscope*

The working electrode (WE) after the electrochemical experiment was removed from the cell. It was then left to dry in a vertical position in the same way as when it was in the electrochemical cell during the experiment. This position was chosen to reduce pooling and drying of unattached microbes. Olympus Compound Microscope BH2-RFCA and ImageJ were used to monitor the changes in bacterial cells percentage coverage over the clay-modified ITO electrodes.

### *2.7 Scanning Electron Microscopy (SEM)*

*S. oneidensis* MR-1 attached on the modified electrodes were imaged using an SEM (HITACHI, SU3500). The clay-modified ITO after the electrochemical experiment was fixed with 2.5% glutaraldehyde for 2 h, rinsed three times in phosphate buffer (pH 7.0, 50 mM), dehydrated by alcoholic series (60, 70, 80, 90, 95, and 100%), and then air-dried.[29]

## *3. Results and discussion*

**Table 1.** Composition and formula of clays

| Clay | Name | Formula[30] | %$Fe_2O_3$[30] | CEC meq/100g |
|---|---|---|---|---|
| NAu-1 | Nontronite | $M^+(1.0)$ $[Al_{.58}$ $Fe_{3.38}$ $Mg_{0.05}]$ $[Si_{7.00}$ $Al_{1.00}]$ $O_{20}(OH)_4$ | 34.19 | 74.7[31] |
| SWy-1 | Montmorillonite (Wyoming) | $M^+(0.49)$ $[Al_{3.01}$ Fe $(III)_{0.41}$ $Mn_{0.01}$ $Mg_{.54}Ti_{0.02}]$ $[Si_{7.98}$ $Al_{0.02}]$ $O_{20}(OH)_4$ | 3.35 | 76.4[30] |
| SYn-1 | Synthetic montmorillonite | $M^+(0.22)$ $[Al_{3.99}$ Fe $(III)_{tr}$ $Mn_{tr}$ $Ti_{tr}]$ $[Si_{6.50}$ $Al_{1.50}]$ $O_{20}(OH)_4$ | 0.02 | 70.0[30] |

### 3.1 *Characterization of the clay-modified ITO electrode*

#### 3.1.1 *Particle sizes, clay texture, and films thickness*

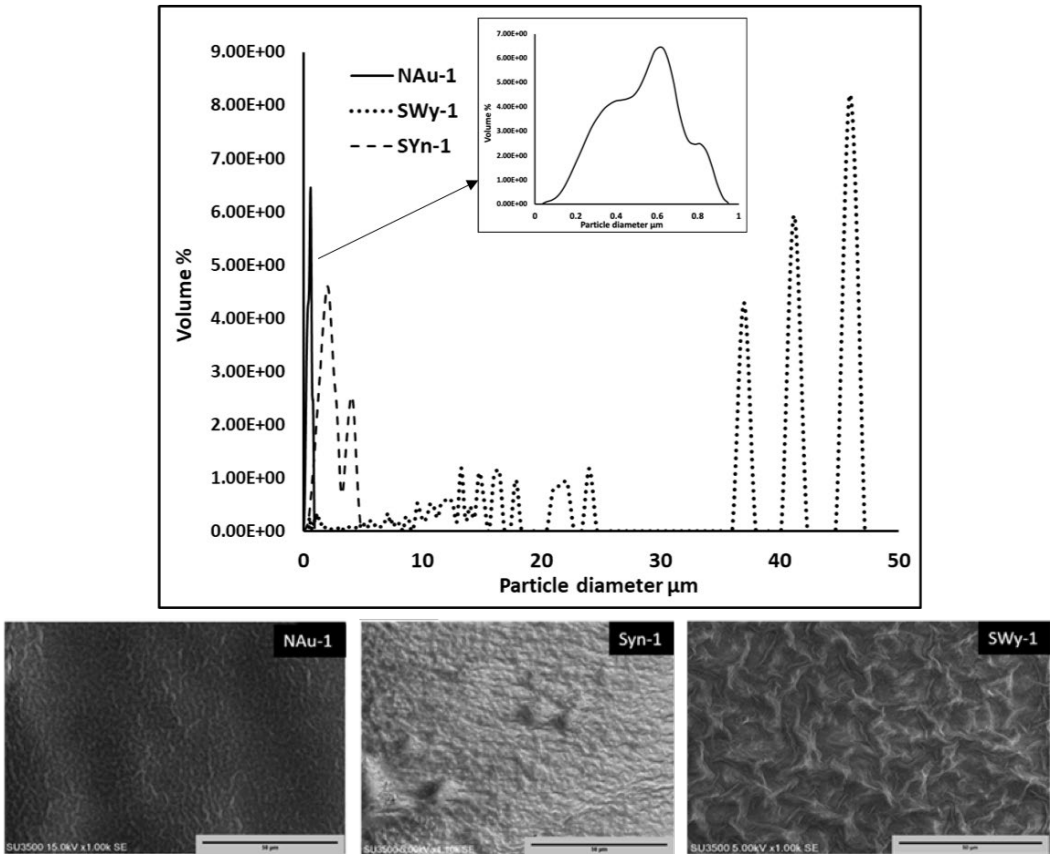


Figure 1. Top particle size distribution of nontronite NAu-1 (solid line), Synthetic montmorillonite SYn-1 (dashed line), and Wyoming SWy-1 (dotted line). Down SEM images for the clay-modified electrodes for each used clay.

Particle sizes of clays affect the absorption[32] and diffusion[33] through the clay layers. (Figure 1 top) shows the particle size distribution of the different clays used in this study. NAu-1 has a particle size of less than 1µm. SYn-1 has a particle size less than 5 µm. SWy-1 shows different particle-size distribution in the range 0.5-50 µm. SYn-1 has a particle size less than 5 µm.

The particle size analyses are consistent with the clay surface texture shown in Figure 1 (down). NAu-1 and SYn-1 appear to have smooth and flat surfaces. SWy-1 shows roughness and bridging surfaces. The cation exchange capacities (CECs) for used clays are similar (74.7, 76.4 and 70.0 meq/100g) (Table 1). The films' thickness measurements were examined by SEM. On each testing sample, the thickness was measured at three different points and the average values were taken. The film thicknesses ranged from 5 to 16 µm thick. Figure 2 demonstrates the film thicknesses for the lowest amounts of each clay placed on the ITO

electrode. NAu-1 and SYn-1 formed compact films whilst SWy-1 created expanded films. The more compact the film is, the more difficult for the species to diffuse through the film. SWy-1 has a higher film thickness (7 μm) than others, which is expected because it has larger particles size.

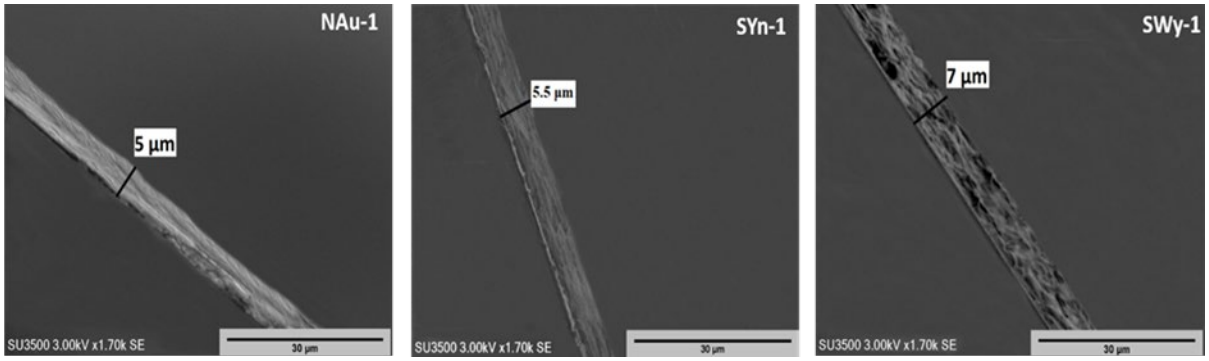


Figure 2. Clay film thickness for each clay for the lowest amount of clay placed on the ITO electrode.

### 3.1.2 *Electrochemical behavior of $Fe(CN)_6$ in clay films: determination of the porosity and coverage of the films*

Clay interlayers expand when exposed to water. Hydrated exchangeable cations force clay layers apart. Coverage and porosity of the films can be examined using the $[Fe(CN)_6]^{3-}$. This electrochemically active ion was chosen as it is negatively charged forcing it to move through the larger pores of the film.[34] Currents measured were recorded as a ratio of the current at the clay-modified ITO electrode to the bare ITO electrode. The changes in the ratio reflect the changes in the interlayer spacing through the clay film.[35]

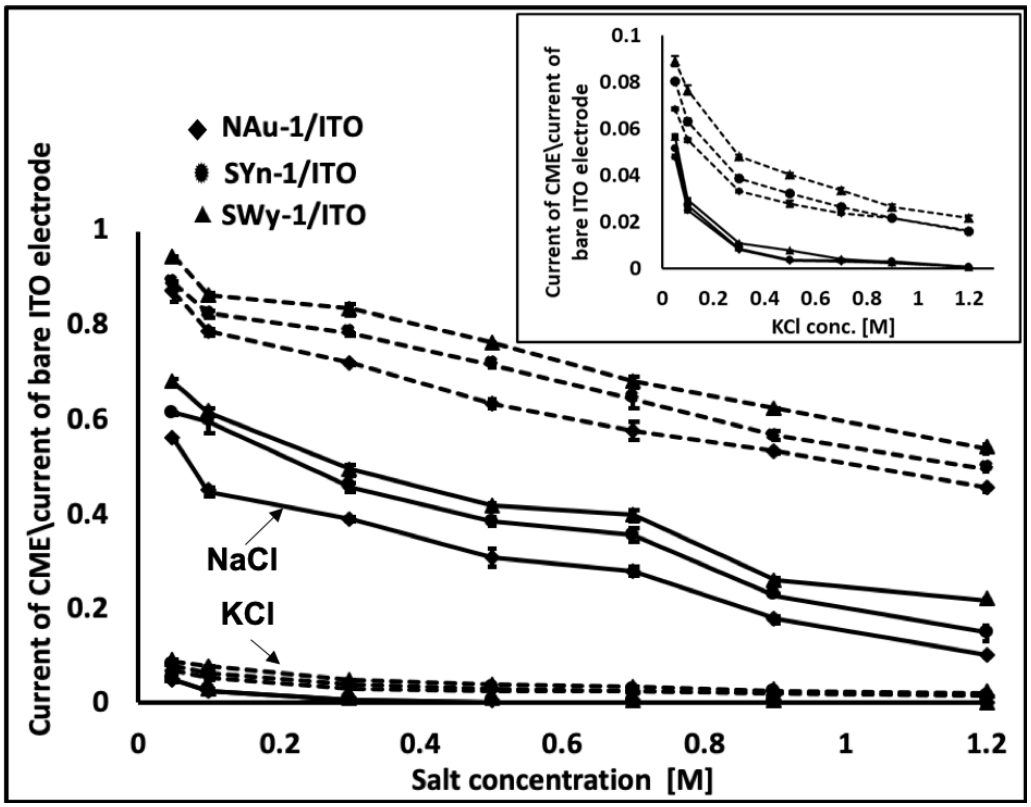


Figure 3. Ratio current for the three used clays as a function of electrolyte concentration and type, (--) represent the lowest film thickness (—) represent the highest film thickness for each clay.

Figure 3 shows the relationship between the ratio of the reduction current using different NaCl concentration at the lowest and highest clay film thicknesses. As expected, the ratio was highest at the lowest film thicknesses (dashed line) indicating clay covered less of the surface. The ratio was 0.94, 0.89, and 0.87 for montmorillonite SWy-1, SYn-1 and NAu-1, respectively. As the concertation of NaCl increased, the ratio, at this low clay thickness decreased until it became 0.54, 0.50, and 0.46 for montmorillonite SWy-1, SYn-1 and NAu-1, respectively. The ratio at the highest clay film thickness (solid line) was lower than at the lower clay film thickness, consistent with greater surface coverage. The ratio was 0.68, 0.61, and 0.56 for montmorillonite SWy-1, SYn-1 and NAu-1, respectively. As the concertation of NaCl to 1.2 M increased, the ratio decreased until it became 0.22, 0.14, and 0.10 for montmorillonite SWy-1, SYn-1 and NAu-1, respectively.

At the low salt concentration, the interlayer expanded, which caused an increase in the pore space, allowing for more diffusion for the probe ion. Increasing the salt concentration compacted the interlayer, which caused decreases in the pore space, so less diffusion of the probe ion took place. $Na^+$ cations required high hydration energy to be dehydrated so they could enter the interlayer in their hydrated form. Those cations in the hydrated form forced apart the clay layers. Soaking clay with different concentrations of KCl, on the other hand, creates compact layers. $K^+$ cations are easily dehydrated and have low hydration energy compare to $Na^+$.[35] KCl soaked clays should therefore have lower porosities. A value of $R \leq 0.04$ can be considered to be complete coverage of the surface.[36] R values for both the lower and higher film thicknesses in the presence of KCl were less than 0.02 at 1.2 M of KCl As shown in Figure 3. This indicated that the clay completely covered the ITO electrode.

All clays, regardless of particle size (NAu-1<SYn-1<SWy-1), showed decreasing porosity with higher salt concentration and in the presence of KCl. However, porosity was also affected by particle size. The particle size findings shown in Figure 1 and the probe ion experiments in Figure 3 proved that, as the particle size decreased the porosity became smaller and therefore diffusion decreased.

### 3.2 *Clay-modified ITO electrode with Oneidensis Shewanella MR-1*

#### *3.2.1 Chronoamperometry*

The current density as a function of time during the loading process at +0.2 V is shown in Figure 4 (A). For the experiment shown, the thickest clay films were used. The maximum current density obtained by NAu-1/ITO electrode was ($1.40 \pm 0.0015$ μA $cm^{-2}$) which is about 19 times higher than the bare ITO electrode ($0.07 \pm 0.0013$ μA $cm^{-2}$). The maximum current density obtained by SWy-1/ITO electrode was ($0.26 \pm 0.0014$ μA $cm^{-2}$) which is about 3 times higher than the bare ITO electrode. There was no current obtained with SYn-1/ITO electrode.

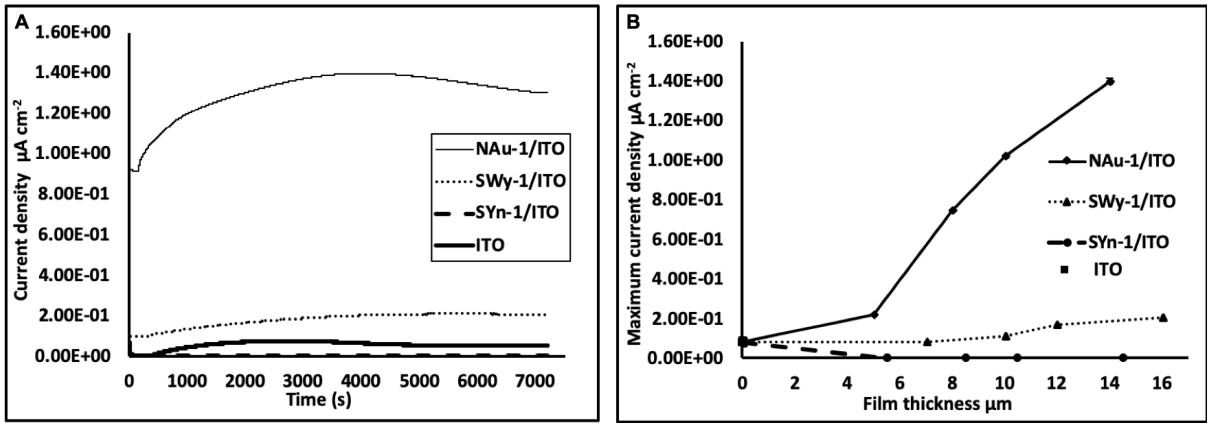


**Figure 4.** Current density as a function of time generated by *Shewanella oneidensis MR-1* on the clay-modified ITO electrodes poised at +0.2 V at the thickest film of each clay (A). The changing in current densities in the presence of the three clays with multi-film thicknesses (B).

Figure 3 demonstrated that increasing film thickness decreased porosity. This would indicate that thick clay films should inhibit charge transfer from bacteria to the underlying clay surface. Contrasting results were observed for iron containing clays (NAu-1/ITO and SWy-1) (Figure 4B). The maximum current density increased when increasing the clay film thickness in both NAu-1/ITO, and SWy-1/ITO. Increasing the film thickness in SYn-1 did not change the current density. This suggests that the increase in current density may be caused by iron mediated charge transfer. The increase in the maximum current density with thickness is significantly much higher when utilizing the NAu-1/ITO electrode compared to the SWy-1/ITO electrode. The effect of increasing the film thickness of NAu-1/ITO on the surface was of the order of 3/1.

As shown in Table 1, NAu-1 is iron rich clay so it contains more amount of $Fe^{3+}$ in the octahedral sheet than the SWy-1 clay. The SYn-1 clay contains non-iron and it did not produce any current, which may be further evidence that the electron transfers occurred thru $Fe^{3+}$ in the clay. Most of the structural iron in clay is ferric iron that can be reduced biologically by metal reducing bacteria, which has been proved by several studies.[37-40] Structural $Fe^{3+}$ in clay acts as an electron acceptor and the organic matter in the growth media serves as an electron donor. In the bio-reduction process, metal-reducing bacteria attach themselves to the clay surface.[13] Microorganisms reduce structural $Fe^{3+}$ in clay to $Fe^{2+}$ [37-38, 41] which can be re-oxidized by

pollutants such as chlorinated solvents, nitroaromatic explosives[42-44], and metals such as U, Tc, Cr.[45-47]At least 90% of the structural $Fe^{2+}$ can be re-oxidized to $Fe^{3+}$.[48-49] *Shewanella O.* MR-1 contains cytochromes in the outer membrane.[50-53] An attractive force between S. oneidensis whole cells and hematite surfaces was detected.[54] Moreover, there was specific bonding detected between MtrC and hematite surfaces.[55] There is a direct attraction between OM C-type cytochromes and $Fe^{3+}$ and localization of the cytochromes on the cell surface. MtrC thus localized to interface between *S. oneidensis* cells and hematite during $Fe^{3+}$ reduction.[56-57]

An alternative hypothesis might be proposed. The cell wall of the bacteria is partially negatively charged and partially lipid in character. Thus, it could anticipate that bacteria are more greatly attached to surfaces with both characteristics. Hydrophilicity can be measured by contact angle, $\theta_c$. The hydrophilicity of the bare electrode is low as $\theta_c$ of the bare ITO electrode was ~ 70.0° was large. The contact angle for the clays varied, but not in the order consistent with the obtained currents densities in Figure 4. The currents densities were in the order NAu-1/ITO > SWy-1/ITO > SYn-1/ITO while the contact angles were SWy-1/ITO (~30.0°) > SYn-1/ITO (~20.0°)> NAu-1/ITO (~15°C). Syn-1 with the lowest improved performance increased the hydrophilicity more so than did SWy-1. This suggests that iron content is a larger driving force than hydrophilicity.

### *3.2.2 Cyclic voltammetry (CV) and electric charge (Q)*

After being poised at +0.2 V for 2 hours, the cyclic voltammetry of the clay-modified ITO electrodes was recorded. Figure 5 (A) shows the cyclic voltammetry of NAu-1/ITO, SWy-1/ITO, SYn-1/ITO, and the bare ITO electrode. The redox peaks with midpoint potential of (-0.19 V) which is consistent with that of the outer membrane Cyts-c. The potential range for OM Cyts-c is in a wide potential range from 0.13 V to -0.27 V.[58-59]

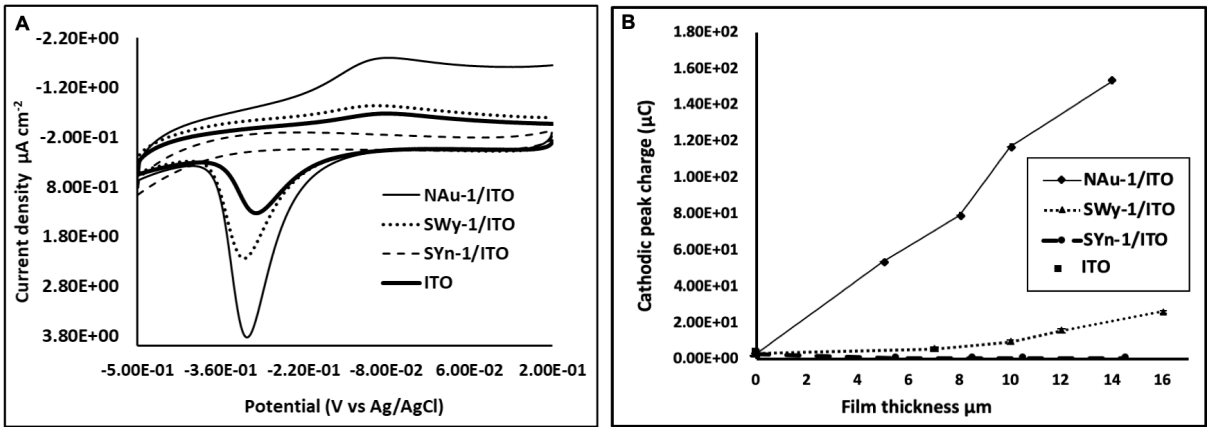


**Figure 5.** (A) Cyclic voltammetry (CV) of the clay-modified ITO electrode after 2 hours of chronoamperometry at scan rate of 5 mV/S with the highest film thickness of each clay (B) the cathodic peak charge (Q) versus the film thickness of each clay-modified electrode

The results of the cyclic voltammetry experiments are consistent with the chronoamperometry experiments in Figure 4. The NAu-1/ITO electrode achieved the highest reduction peak's current density (3.84 ±0.15 µA $cm^{-2}$). The SWy-1/ITO electrode recorded reduction peak's current density of (2.26 ± 0.34 µA $cm^{-2}$). The reduction peak current density of the bare ITO was (1.33 ± 0.06 µA $cm^{-2}$). There was no reduction peak current density obtained with SYn-1/ITO.

Figure 5 (B) represents the total quantity of electric charge (Q) versus the film thickness of each clay type. Q was calculated by integrating the area under the reduction peak in the cyclic voltammetry using the following equation [60-61]

$$Q = \int_0^t Idt$$

I is the current and t is the working time. The black square in the Figure 5 (B) represents the Q value using the bare ITO electrode, which is (2.95 ± 0.4 µC). The Q values obtained at the highest film thickness of NAu-1/ITO and SWy-1/ITO were (153.58 ±1.2 µC, and 25.84 ±0.9 µC) respectively. There was no Q value for the non-iron clay SYn-1/ITO. Again, these results are consistent with the chronoamperometry experiments discussed above.

### 7.2.3 *SEM images and area coverage percentage by confocal microscope*

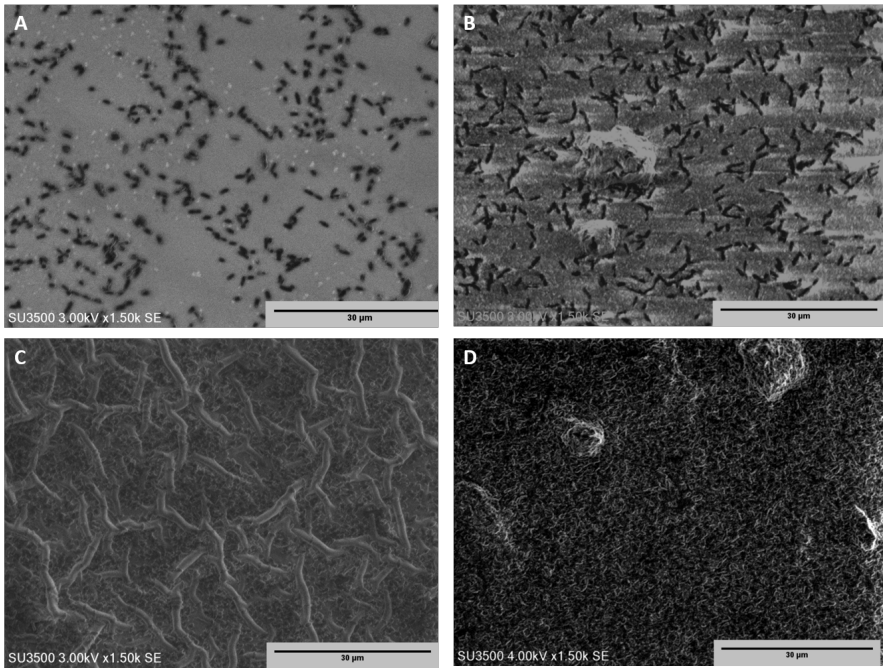


**Figure 6.** SEM for *S. Oneidensis* MR-1 attached to (A) bare ITO electrode (B) SYn-1/ITO electrode (C) SWy-1/ITO electrode (D) NAu-1/ITO electrode

Figure 6 shows the SEM for the attached bacterial cells on the clay-modified ITO electrode at the thickest film of each clay. As shown in the images, bacterial cells attached to the clay surface. In Figure 6 the bare ITO (A) and SYn-1/ITO (B) showed about 30% and 29% coverage, respectively. The SWy-1/ITO (C) electrode achieved more coverage, with about 43%. The iron rich clay NAu-1/ITO electrode showed the highest bacterial cells coverage, which was about 86%.

A relationship was found between the maximum current density obtained by *S. oneidensis* MR-1 and the area coverage percentage of bacterial cells on the clay-modified ITO electrodes as shown in Figure 7. The coverage percentage for the bare ITO (black square) was about 30% was used as a comparison.

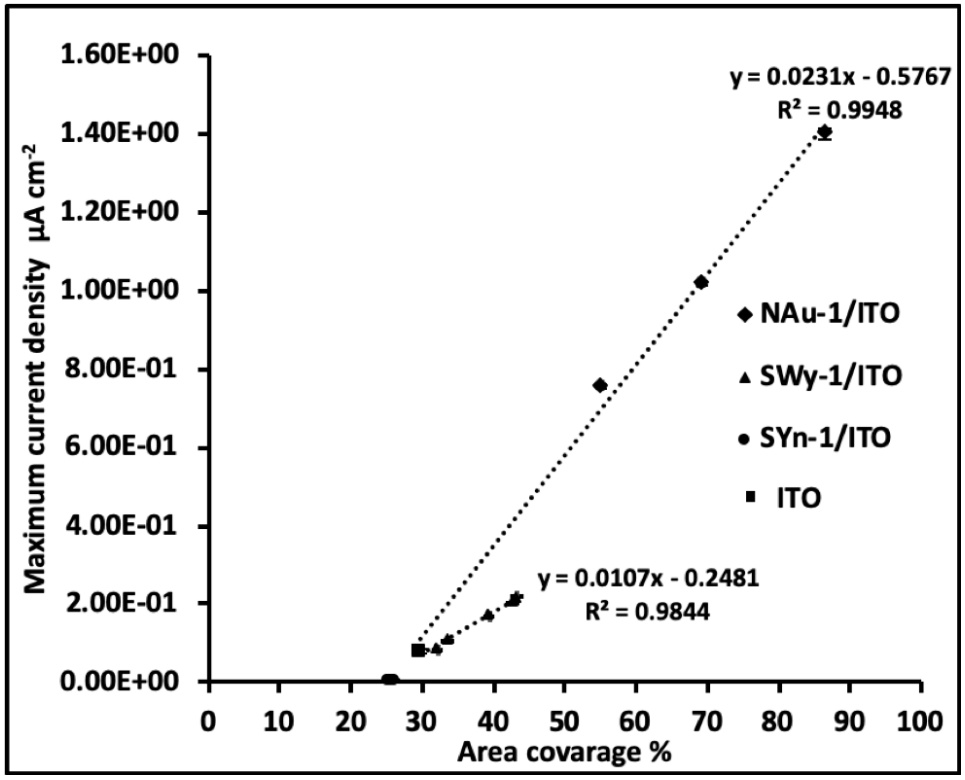


**Figure 7.** Maximum current density obtained by *S. oneidensis* MR-1 at multiple film thicknesses of each clay type vs. the area coverage % of bacterial cells on the clay-modified ITO electrode

The increase in the coverage percentage was highest with NAu-1/ITO compared to the SWy1/ITO, as it appears in the difference slopes of the two lines.As shown in Table 1, NAu-1 has more iron than SWy-1 so the amount of $Fe^{3+}$ available for electron transfer process will be much more in case of NAu-1/ITO electrode allowing for larger bacterial surface coverage. Non-iron clay SYn-1/ITO has coverage percentage of 29%, which is near the coverage percentage of the bare ITO. SYn-1/ITO electrode shows no remarkable difference in the coverage percentage even when there is an increase in the amount of the added clay to the electrode. This results clearly indicate that $Fe^{3+}$ in the clay not only increased the electron transfer process but also attracts bacterial cells to attach to the electrode. These findings indicate that there is a direct relationship between the current density obtained and the bacterial cells attached to the electrode. Therefore, as more bacterial cells arrived and attached to the electrode surface, the current produced will be higher.

## 4. Conclusion

In summary, the ferricyanide experiments proved that the clay-modified ITO electrodes were successfully prepared in the present study. Particle sizes, porosity, coverage, and film thicknesses of each used clay were examined. The ferricyanide experiments showed that increasing the film thickness of the CME decreased the diffusion of the ferricyanide anion. The clay-modified ITO electrodes show different results when utilized with *Shewanella O.* MR-1. Increasing the film thicknesses of NAu-1/ITO and SWy-1/ITO results in an increase in current densities, reduction peak current, and bacterial cell attachment. In the case of SYn-1/ITO, increasing the film thickness did not yield any difference in the results. NAu-1 and SWy-1 both contain iron, which transfers electrons to the ITO. The iron clay-modified electrode technique could be a promising modification method to use in microbial fuel cells. It is an unexpansive and nonchemical method.

***Acknowledgments***

This research utilized a scanning electron microscope, which was funded by the NSF, Major Research Instrumentation (MRI) Program via Award No. 1726994.

References

1. Wu, W.; Lesnik, K. L.; Xu, S.; Wang, L.; Liu, H., Impact of tobramycin on the performance of microbial fuel cell. *Microbial Cell Factories* **2014,** *13* (1), 91.
2. Abourached, C.; English, M. J.; Liu, H., Wastewater treatment by Microbial Fuel Cell (MFC) prior irrigation water reuse. *Journal of Cleaner Production* **2016,** *137*, 144-149.
3. Liu, H.; Ramnarayanan, R.; Logan, B. E., Production of electricity during wastewater treatment using a single chamber microbial fuel cell. *Environmental science & technology* **2004,** *38* (7), 2281-2285.
4. Cecconet, D.; Callegari, A.; Capodaglio, A., Bioelectrochemical systems for removal of selected metals and perchlorate from groundwater: A review. *Energies* **2018,** *11* (10), 2643.
5. Baron, D.; LaBelle, E.; Coursolle, D.; Gralnick, J. A.; Bond, D. R., Electrochemical measurement of electron transfer kinetics by Shewanella oneidensis MR-1. *Journal of biological chemistry* **2009,** *284* (42), 28865-28873.
6. Liao, Z.-H.; Sun, J.-Z.; Sun, D.-Z.; Si, R.-W.; Yong, Y.-C., Enhancement of power production with tartaric acid doped polyaniline nanowire network modified anode in microbial fuel cells. *Bioresource technology* **2015,** *192*, 831-834.
7. Pant, D.; Van Bogaert, G.; Diels, L.; Vanbroekhoven, K., A review of the substrates used in microbial fuel cells (MFCs) for sustainable energy production. *Bioresource technology* **2010,** *101* (6), 1533-1543.
8. Zhang, C.; Zhang, D.; Xiao, Z., Application of Redox Mediators in Bioelectrochemical System. In *Bioelectrochemistry Stimulated Environmental Remediation*, Springer: 2019; pp 205-226.
9. Logan, B. E.; Wallack, M. J.; Kim, K.-Y.; He, W.; Feng, Y.; Saikaly, P. E., Assessment of microbial fuel cell configurations and power densities. *Environmental Science & Technology Letters* **2015,** *2* (8), 206-214.
10. Wu, W.; Niu, H.; Yang, D.; Wang, S.-B.; Wang, J.; Lin, J.; Hu, C., Controlled Layer-By-Layer Deposition of Carbon Nanotubes on Electrodes for Microbial Fuel Cells. *Energies* **2019,** *12* (3), 363.
11. Ji, J.; Jia, Y.; Wu, W.; Bai, L.; Ge, L.; Gu, Z., A layer-by-layer self-assembled Fe2O3 nanorod-based composite multilayer film on ITO anode in microbial fuel cell. *Colloids and Surfaces A: Physicochemical and Engineering Aspects* **2011,** *390* (1-3), 56-61.
12. Zhu, Y.; Ji, J.; Ren, J.; Yao, C.; Ge, L., Conductive multilayered polyelectrolyte films improved performance in microbial fuel cells (MFCs). *Colloids and Surfaces A: Physicochemical and Engineering Aspects* **2014,** *455*, 92-96.
13. Dong, H., Clay–microbe interactions and implications for environmental mitigation. *Elements* **2012,** *8* (2), 113-118.
14. Beall, G. W., The use of organo-clays in water treatment. *Applied Clay Science* **2003,** *24* (1-2), 11-20.
15. Fitch, A., *Electrochemical Properties of Clays*. The Clay Minerals Society: 2002; Vol. 10.
16. An, N.; Zhou, C. H.; Zhuang, X. Y.; Tong, D. S.; Yu, W. H., Immobilization of enzymes on clay minerals for biocatalysts and biosensors. *Applied Clay Science* **2015,** *114*, 283-296.
17. Unal, B.; Yalcinkaya, E. E.; Demirkol, D. O.; Timur, S., An electrospun nanofiber matrix based on organo-clay for biosensors: PVA/PAMAM-Montmorillonite. *Applied Surface Science* **2018,** *444*, 542-551.
18. Mousty, C., Sensors and biosensors based on clay-modified electrodes—new trends. *Applied Clay Science* **2004,** *27* (3-4), 159-177.

19. Zen, J.-M.; Kumar, A. S., Peer reviewed: the prospects of clay mineral electrodes. ACS Publications: 2004.
20. Yao, K.; Shimazu, K.; Nakata, M.; Yamagishi, A., Clay-modified electrodes as studied by the quartz crystal microbalance: adsorption of ruthenium complexes. *Journal of Electroanalytical Chemistry* **1998,** *442* (1-2), 235-242.
21. Yao, K.; Taniguchi, M.; Nakata, M.; Shimazu, K.; Takahashi, M.; Yamagishi, A., Mass transport on an anionic clay-modified electrode as studied by a quartz crystal microbalance. *Journal of Electroanalytical Chemistry* **1998,** *457* (1-2), 119-128.
22. Xiang, Y.; Villemure, G., Electron transport in clay-modified electrodes: study of electron transfer between electrochemically oxidized tris (2, 2′-bipyridyl) iron cations and clay structural iron (II) sites. *Canadian Journal of Chemistry* **1992,** *70* (6), 1833-1837.
23. Xiang, Y.; Villemure, G., Electrodes modified with synthetic clay minerals: evidence of direct electron transfer from structural iron sites in the clay lattice. *Journal of Electroanalytical Chemistry* **1995,** *381* (1-2), 21-27.
24. Lei, C.; Lisdat, F.; Wollenberger, U.; Scheller, F. W., Cytochrome c/Clay-Modified Electrode. *Electroanalysis: An International Journal Devoted to Fundamental and Practical Aspects of Electroanalysis* **1999,** *11* (4), 274-276.
25. Charradi, K.; Forano, C.; Prevot, V.; Ben Haj Amara, A.; Mousty, C., Direct electron transfer and enhanced electrocatalytic activity of hemoglobin at iron-rich clay modified electrodes. *Langmuir* **2009,** *25* (17), 10376-10383.
26. Charradi, K.; Gondran, C.; Amara, A. B. H.; Prevot, V.; Mousty, C., H2O2 determination at iron-rich clay modified electrodes. *Electrochimica Acta* **2009,** *54* (17), 4237-4244.
27. Koffi, O.; Bile, B.; Bengourram, J.; Tankiouine, S.; Latrache, H., Electrochemical study of interaction of bacteria and clay. *J Microb Biochem Technol* **2016,** *8*, 060-064.
28. Yao, K.; Shimazu, K.; Nakata, M.; Yamagishi, A., Clay-modified electrodes as studied by the quartz crystal microbalance: redox processes of ruthenium and iron complexes. *Journal of Electroanalytical Chemistry* **1998,** *443* (2), 253-261.
29. Wu, W.; Yang, F.; Liu, X.; Bai, L., Influence of substrate on electricity generation of Shewanella loihica PV-4 in microbial fuel cells. *Microbial cell factories* **2014,** *13* (1), 69.
30. Fripiat, H. V. O. a. J. J., SOURCE CLAY PHYSICAL/CHEMICAL DATA. **May 2019**.
31. Koo, T.-h.; Jang, Y.-n.; Kogure, T.; Kim, J. H.; Park, B. C.; Sunwoo, D.; Kim, J.-w., Structural and chemical modification of nontronite associated with microbial Fe (III) reduction: indicators of “illitization”. *Chemical Geology* **2014,** *377*, 87-95.
32. Tsai, W.; Lai, C.; Hsien, K., Effect of particle size of activated clay on the adsorption of paraquat from aqueous solution. *Journal of colloid and interface science* **2003,** *263* (1), 29-34.
33. Kozaki, T.; Sato, Y.; Nakajima, M.; Kato, H.; Sato, S.; Ohashi, H., Effect of particle size on the diffusion behavior of some radionuclides in compacted bentonite. *Journal of Nuclear Materials* **1999,** *270* (1-2), 265-272.
34. Stein, J. A.; Fitch, A., Effect of clay type on the diffusional properties of a clay-modified electrode. *Clays and clay minerals* **1996,** *44* (3), 381-392.
35. Fitch, A.; Du, J.; Gan, H.; Stucki, J. W., Effect of clay charge on swelling: A clay-modified electrode study. *Clays and clay minerals* **1995,** *43* (5), 607-614.
36. Macha, S.; Zayia, G.; Du, J.; Stein, J.; Fitch, A., Diffusion control in thin clay films: tailoring layered clay film structures through control of aqueous electrolyte. *Applied clay science* **1999,** *15* (1-2), 153-172.
37. Kostka, J. E.; Dalton, D. D.; Skelton, H.; Dollhopf, S.; Stucki, J. W., Growth of iron (III)-reducing bacteria on clay minerals as the sole electron acceptor and comparison of

growth yields on a variety of oxidized iron forms. *Appl. Environ. Microbiol.* **2002,** *68* (12), 6256-6262.
38. Stucki, J. W.; Komadel, P.; Wilkinson, H. T., Microbial Reduction of Structural Iron (III) in Smectites 1. *Soil Science Society of America Journal* **1987,** *51* (6), 1663-1665.
39. Kostka, J. E.; Wu, J.; Nealson, K. H.; Stucki, J. W., The impact of structural Fe (III) reduction by bacteria on the surface chemistry of smectite clay minerals. *Geochimica et Cosmochimica Acta* **1999,** *63* (22), 3705-3713.
40. Dong, H.; Kukkadapu, R. K.; Fredrickson, J. K.; Zachara, J. M.; Kennedy, D. W.; Kostandarithes, H. M., Microbial reduction of structural Fe (III) in illite and goethite. *Environmental Science & Technology* **2003,** *37* (7), 1268-1276.
41. Schaefer, M. V.; Gorski, C. A.; Scherer, M. M., Spectroscopic evidence for interfacial Fe (II)− Fe (III) electron transfer in a clay mineral. *Environmental Science & Technology* **2010,** *45* (2), 540-545.
42. Hofstetter, T. B.; Neumann, A.; Schwarzenbach, R. P., Reduction of nitroaromatic compounds by Fe (II) species associated with iron-rich smectites. *Environmental Science & Technology* **2006,** *40* (1), 235-242.
43. Lee, W.; Batchelor, B., Reductive capacity of natural reductants. *Environmental science & technology* **2003,** *37* (3), 535-541.
44. Neumann, A.; Hofstetter, T. B.; Skarpeli-Liati, M.; Schwarzenbach, R. P., Reduction of polychlorinated ethanes and carbon tetrachloride by structural Fe (II) in smectites. *Environmental science & technology* **2009,** *43* (11), 4082-4089.
45. Brigatti, M. F.; Franchini, G.; Lugli, C.; Medici, L.; Poppi, L.; Turci, E., Interaction between aqueous chromium solutions and layer silicates. *Applied Geochemistry* **2000,** *15* (9), 1307-1316.
46. Ilton, E. S.; Haiduc, A.; Moses, C. O.; Heald, S. M.; Elbert, D. C.; Veblen, D. R., Heterogeneous reduction of uranyl by micas: Crystal chemical and solution controls. *Geochimica et Cosmochimica Acta* **2004,** *68* (11), 2417-2435.
47. Peretyazhko, T.; Zachara, J. M.; Heald, S. M.; Jeon, B.-H.; Kukkadapu, R. K.; Liu, C.; Moore, D.; Resch, C. T., Heterogeneous reduction of Tc (VII) by Fe (II) at the solid–water interface. *Geochimica et Cosmochimica Acta* **2008,** *72* (6), 1521-1539.
48. Lee, K.; Kostka, J. E.; Stucki, J. W., Comparisons of structural Fe reduction in smectites by bacteria and dithionite: An infrared spectroscopic study. *Clays and Clay Minerals* **2006,** *54* (2), 195-208.
49. Ribeiro, F. R.; Fabris, J. D.; Kostka, J. E.; Komadel, P.; Stucki, J. W., Comparisons of structural iron reduction in smectites by bacteria and dithionite: II. A variable-temperature Mössbauer spectroscopic study of Garfield nontronite. *Pure and Applied Chemistry* **2009,** *81* (8), 1499-1509.
50. Neumann, A.; Petit, S.; B. Hofstetter, T., *Evaluation of redox-active iron sites in smectites using middle and near infrared spectroscopy*. 2011; Vol. 75, p 2336-2355.
51. Claire, F.; Huo, D.; Yan, L.; Wu, J.; Stucki, J., *Infrared study of reduced and reduced-reoxidized ferruginous smectite*. 2002; Vol. 50, p 455-469.
52. Claire, F.; Huo, D.; Yan, L.; Wu, J.; Stucki, J., *Effect of Fe oxidation state on the IR spectra of Garfield nontronite*. 2002; Vol. 87, p 630-641.
53. Yan, L.; Stucki, J., *Effects of Structural Fe Oxidation State on the Coupling of Interlayer Water and Structural Si−O Stretching Vibrations in Montmorillonite*. 1999; Vol. 15, p 4648-4657.
54. Lower, S. K.; Hochella, M. F., Jr.; Beveridge, T. J., Bacterial recognition of mineral surfaces: nanoscale interactions between Shewanella and alpha-FeOOH. *Science (New York, N.Y.)* **2001,** *292* (5520), 1360-3.

55. Lower, B. H.; Shi, L.; Yongsunthon, R.; Droubay, T. C.; McCready, D. E.; Lower, S. K., Specific bonds between an iron oxide surface and outer membrane cytochromes MtrC and OmcA from Shewanella oneidensis MR-1. *Journal of bacteriology* **2007,** *189* (13), 4944-52.
56. Lower, B. H.; Yongsunthon, R.; Shi, L.; Wildling, L.; Gruber, H. J.; Wigginton, N. S.; Reardon, C. L.; Pinchuk, G. E.; Droubay, T. C.; Boily, J. F.; Lower, S. K., Antibody recognition force microscopy shows that outer membrane cytochromes OmcA and MtrC are expressed on the exterior surface of Shewanella oneidensis MR-1. *Appl Environ Microbiol* **2009,** *75* (9), 2931-5.
57. Reardon, C. L.; Dohnalkova, A. C.; Nachimuthu, P.; Kennedy, D. W.; Saffarini, D. A.; Arey, B. W.; Shi, L.; Wang, Z.; Moore, D.; McLean, J. S.; Moyles, D.; Marshall, M. J.; Zachara, J. M.; Fredrickson, J. K.; Beliaev, A. S., Role of outer-membrane cytochromes MtrC and OmcA in the biomineralization of ferrihydrite by Shewanella oneidensis MR-1. *Geobiology* **2010,** *8* (1), 56-68.
58. Kim, B. H.; Kim, H. J.; Hyun, M. S.; Park, D. H., Direct electrode reaction of Fe (III)-reducing bacterium, Shewanella putrefaciens. *Journal of Microbiology and Biotechnology* **1999,** *9*, 127-131.
59. Meitl, L. A.; Eggleston, C. M.; Colberg, P. J. S.; Khare, N.; Reardon, C. L.; Shi, L., Electrochemical interaction of Shewanella oneidensis MR-1 and its outer membrane cytochromes OmcA and MtrC with hematite electrodes. *Geochimica et Cosmochimica Acta* **2009,** *73* (18), 5292-5307.
60. Ji, J.; Jia, Y.; Wu, W.; Bai, L.; Ge, L.; Gu, Z., A layer-by-layer self-assembled Fe2O3 nanorod-based composite multilayer film on ITO anode in microbial fuel cell. *Colloids and Surfaces A: Physicochemical and Engineering Aspects* **2011,** *390* (1), 56-61.
61. Wu, W.; Yang, F.; Liu, X.; Bai, L., *Influence of substrate on electricity generation of Shewanella loihica PV-4 in microbial fuel cells*. 2014; Vol. 13, p 69.